



## RESEARCH ARTICLE

10.1002/2015JC011075

## Could the Madagascar bloom be fertilized by Madagascar iron?

M. A. Srokosz<sup>1</sup>, J. Robinson<sup>2</sup>, H. McGrain<sup>2</sup>, E. E. Popova<sup>1</sup>, and A. Yool<sup>1</sup><sup>1</sup>National Oceanography Centre, University of Southampton Waterfront Campus, Southampton, UK, <sup>2</sup>Ocean and Earth Science, National Oceanography Centre Southampton, University of Southampton, UK

## Key Points:

- Madagascar iron can be advected east to fertilize the late austral summer bloom
- Lagrangian particle tracking shows that mesoscale eddies cause the advection
- interannual variability in the bloom is caused by eddy variability

## Correspondence to:

M. A. Srokosz,  
mas@noc.ac.uk

## Citation:

Srokosz, M. A., J. Robinson, H. McGrain, E. E. Popova, and A. Yool (2015), Could the Madagascar bloom be fertilized by Madagascar iron?, *J. Geophys. Res. Oceans*, 120, 5790–5803, doi:10.1002/2015JC011075.

Received 24 JUN 2015

Accepted 29 JUL 2015

Accepted article online 4 AUG 2015

Published online 21 AUG 2015

**Abstract** In the oligotrophic waters to the east of Madagascar, a large phytoplankton bloom is found to occur in late austral summer. This bloom is composed of nitrogen fixers and can cover up to ~1% of the world's ocean surface area. Satellite observations show that its spatial structure is closely tied to the underlying mesoscale eddy field in the region. The causes of the bloom and its temporal behavior (timing of its initiation and termination) and spatial variability are poorly understood, in part due to a lack of in situ observations. Here an eddy resolving 1/12° resolution ocean general circulation model and Lagrangian particle tracking are used to examine the hypothesis that iron from sediments around Madagascar could be advected east by the mesoscale eddy field to fertilize the bloom, and that variability in advection could explain the significant interannual variability in the spatial extent of the bloom. The model results suggest that this is indeed possible and furthermore imply that the bloom could be triggered by warming of the mixed layer, leading to optimal conditions for nitrogen fixers to grow, while its termination could be due to iron exhaustion. It is found that advection of Madagascar iron could resupply the bloom region with this micronutrient in the period between the termination of one bloom and the initiation of the next in the following year.

## 1. Introduction

The area to the east of Madagascar lies in the southwestern Indian Ocean subtropical gyre and biologically is one of the oligotrophic regions of the world's oceans. In the late austral summer, a major phytoplankton bloom develops in this region, which varies from year-to-year both in terms of timing and spatial extent. The bloom is easily observed in ocean color measurement of chlorophyll and is known to be composed of nitrogen fixing phytoplankton [Poulton *et al.*, 2009]. In some years, when fully developed, this late austral summer Madagascar bloom can cover ~1% of the world's ocean surface area. It has been described as one of the strongest examples of interannual variability, with respect to ocean biology, after El Niño [Uz, 2007; Srokosz and Quartly, 2013]. Thus, the Madagascar bloom has a major impact on the biogeochemistry of the Indian Ocean basin [Uz, 2007]. Notably, unlike similar late summer blooms elsewhere in the ocean as documented by Wilson and Qiu [2008], the Madagascar bloom propagates to the east, away from Madagascar. Despite the significance of the bloom, the lack of supporting in situ data has led to uncertainty surrounding the mechanisms of its formation, propagation, and termination.

Longhurst [2001] was the first to describe the seasonal development of this major bloom, using ocean color observations from space (from POLDER and Sea-viewing Wide Field-of-view Sensor (SeaWiFS)). He noted that the bloom typically occurred during the period February to April but was not present every year. Subsequent studies have elucidated various aspects of the bloom [e.g., Srokosz *et al.*, 2004; Uz, 2007; Wilson and Qiu, 2008; Poulton *et al.*, 2009; Huhn *et al.*, 2012; Srokosz and Quartly, 2013], but many questions still remain regarding its nature (see Srokosz and Quartly [2013] for a review of what is currently known about the bloom). Based on limited in situ observations [Poulton *et al.*, 2009; Srokosz and Quartly, 2013], it is known that the bloom is composed of nitrogen fixing phytoplankton: *Trichodesmium* and the diatom *Rhizosolenia clevei* with its symbiont *Richelia intracellularis*. Other notable features of the bloom are that it propagates east away from Madagascar and exhibits significant interannual variability in terms of the timing of its initiation and termination, and also in terms of its spatial extent [Wilson and Qiu, 2008]. In his original study, Longhurst [2001] noted the importance of the mesoscale eddy field in the development of the bloom, describing the bloom's spatial structure as dendritic. Subsequent studies have confirmed the impact of the eddy field

© 2015. The Authors.

This is an open access article under the terms of the Creative Commons Attribution License, which permits use, distribution and reproduction in any medium, provided the original work is properly cited.

on the bloom [e.g., *Huhn et al.*, 2012; *Srokosz and Quartly*, 2013]. Although there have been recent studies of the effect of eddies on chlorophyll in the South Indian Ocean [*Dufois et al.*, 2014; *Gaube et al.*, 2013, 2014], these have been focused more on an area further east toward Australia and on austral winter conditions, so have not address the influence of eddies on the bloom directly.

The reasons for the occurrence of the bloom are unclear. *Uz* [2007] proposed that the bloom was fertilized by riverine iron washed off Madagascar by tropical cyclones and then advected to the east by the ocean circulation, and in particular by the mesoscale eddy field. *Srokosz and Quartly* [2013], while accepting the idea of iron fertilization, questioned the river runoff mechanism as the major Madagascar rivers flow into the Mozambique Channel to the west of Madagascar. Instead, they proposed that iron could be supplied from the sediments from the continental shelves to the east and south of Madagascar. As *Elrod et al.* [2004], *Jeandel et al.* [2011], and *Dale et al.* [2015] show, continental shelf sediments can be a major source of iron to the water column and then by advection to the open ocean. *Srokosz and Quartly* [2013] argued that a similar mechanism had been shown to explain both the Kerguelen and Crozet blooms in the Southern Ocean [*Blain et al.*, 2007; *Pollard et al.*, 2009] and, by analogy, could explain the Madagascar bloom. Unfortunately, unlike the Crozet and Kerguelen studies, there are no iron measurements from the Madagascar region. *Mongin et al.* [2009] used a modeling study to demonstrate that winter advection of iron could explain the Kerguelen bloom and a related approach will be used in this study. The hypothesis here is: iron from sediments around Madagascar is advected east by the mesoscale eddy field to fertilize the bloom, and the variability in the advection explains the significant interannual variability in the spatial extent of the bloom. This hypothesis will be examined using a high-resolution (1/12°) ocean model and Lagrangian particle tracking. Given the importance of the mesoscale eddy field for the development of the bloom [*Longhurst*, 2001], it is crucial to use a truly eddy resolving ocean model for this study [*Marzocchi et al.*, 2015].

In the same region to the east of Madagascar, there is also an annual weak austral spring bloom [see, for example, *Uz*, 2007, Figure 2], which is followed by the development of a deep chlorophyll maximum [*Srokosz and Quartly*, 2013]. This austral spring bloom and the subsequent development of a deep chlorophyll maximum are reproduced in biogeochemical models without an iron component, whereas the late austral summer bloom studied here is not (see discussion by *Srokosz and Quartly* [2013] and references therein). In part, the inability of the models to reproduce the late austral summer bloom is due to the omission of the nitrogen fixing phytoplankton, composing the bloom [*Poulton et al.*, 2009], from the ocean biogeochemical models. An exception is the global model of *Monteiro et al.* [2010] which shows pronounced variability over a year in diazotrophs to the east of Madagascar. However, they do not investigate the Madagascar bloom per se and their model resolution is only 1°, so it does not resolve the mesoscale features that are an important aspect of the bloom. The point to draw from these model results is that if iron is advected east from Madagascar probably not all of it will be used up during the weak austral spring bloom and so some will be available to fertilize the late austral summer bloom, which is the focus of this study.

The paper proceeds as follows: section 2 describes the data and model; section 3 explains the methodology used and gives the results obtained by applying Lagrangian particle tracking to the model output; section 4 discusses other factors that affect the bloom; section 5 gives the conclusions of this study.

## 2. Data and Model Description

### 2.1. Satellite Data

#### 2.1.1. SeaWiFS Chlorophyll

For simplicity and because it provides a uniform data set, here a decade, 1998–2007, of SeaWiFS ocean color observations of chlorophyll for the bloom area are used. The specific products used are the SeaWiFS monthly, level 3 Standard Mapped Images with a 9 km resolution [*NASA*, 2009]. These were obtained from <http://oceandata.sci.gsfc.nasa.gov/SeaWiFS/L3SMI/>. In Figure 1, the SeaWiFS data for the bloom period January to April are plotted for each of the 10 years [cf. *Wilson and Qiu*, 2008, Figure 10]. The interannual variability of the bloom, both in terms of timing and of spatial extent, can be clearly seen over the decade of observations.

One point to note is that the criterion for the existence of a late austral summer bloom in the SeaWiFS ocean color data differs amongst studies. For example, *Uz* [2007] uses a ratio of the mean surface

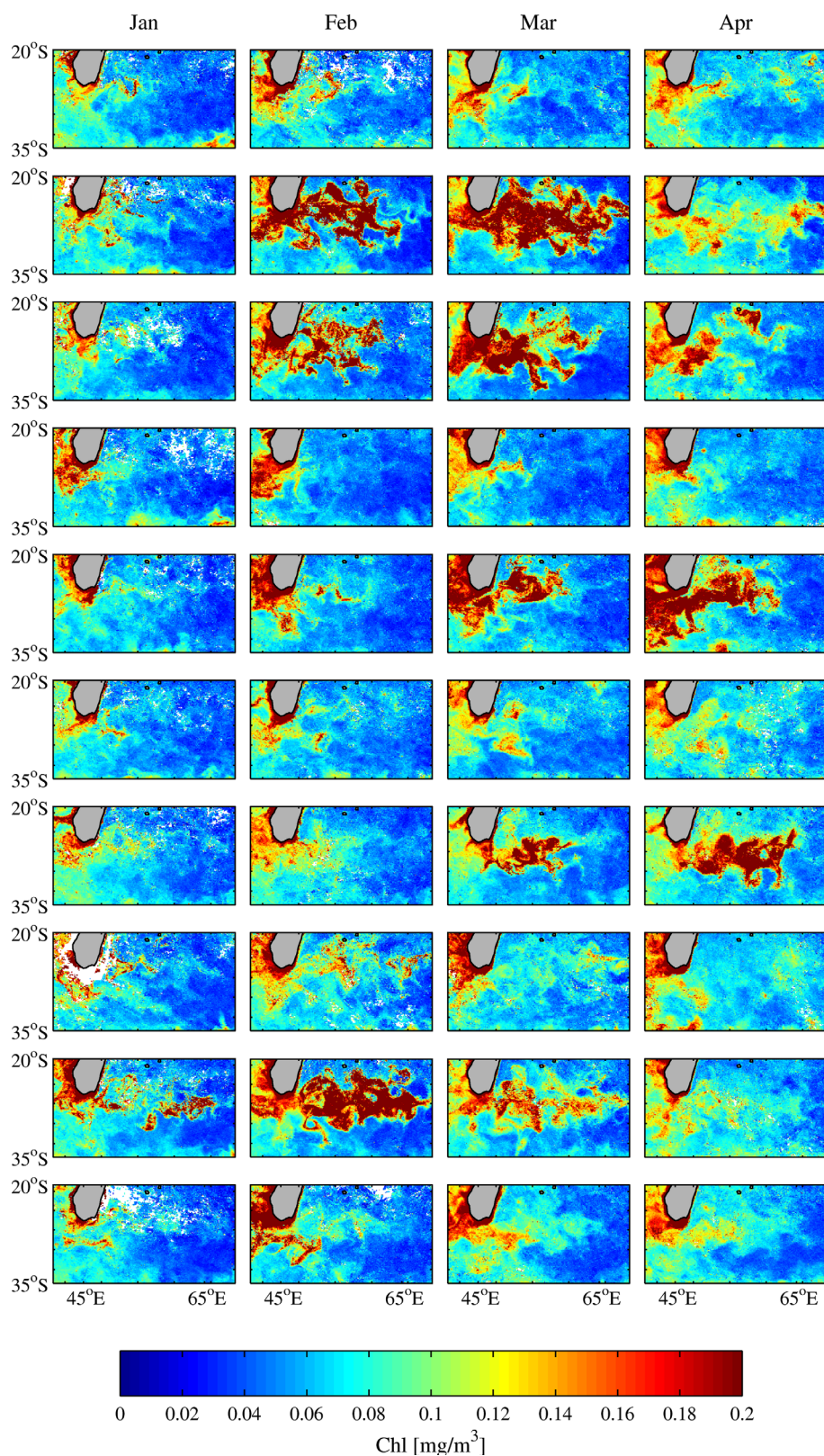


**Figure 1.** SeaWiFS monthly chlorophyll concentration in  $\text{mg chl m}^{-3}$ . Maps for (left to right) January to April for each year (top to bottom) from 1998 to 2007. The interannual variability of both the timing and the spatial extent of the bloom is apparent.

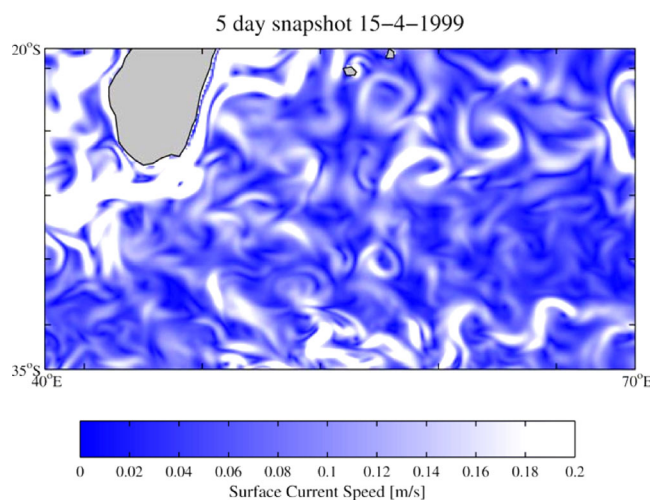


**Figure 2.** NEMO 1/12° model 5 day “snapshot” of the surface current speeds in the Madagascar bloom area, displaying a highly variable mesoscale eddy field that is accord with that seen in observations [cf. Longhurst, 2001, Figure 2]. This illustrates that the high resolution of the NEMO 1/12° model enables it to capture the behavior at the mesoscale that is important for the Madagascar bloom (see also Figure 10 below).

(ADT) is obtained by adding the Sea Level Anomaly to the Mean Dynamic Topography, which is the part of the Mean Sea Surface Height caused by permanent currents (Mean Sea Surface Height minus Geoid). A mapping procedure using optimal interpolation gives ADT maps (MADT or L4 products) at a given date (daily temporal resolution) on  $1/4^\circ \times 1/4^\circ$  spatial grid. Here the sea surface geostrophic velocities computed from the ADT over the period of 1998–2007 are used, to match the SeaWiFS data record.

## 2.2. NEMO Model and Ariane Lagrangian Particle Tracking

The Nucleus for European Modelling of the Ocean (NEMO) model is an ocean general circulation model (GCM). The NEMO 1/12° resolution model has been developed with particular emphasis on realistic representation of fine-scale circulation patterns [Madedec, 2008; Marzocchi *et al.*, 2015] and provides an ideal platform to conduct Lagrangian particle-tracking experiments as it captures the mesoscale behavior, necessary to investigate the Madagascar bloom. The run of the 1/12° NEMO that is used here is that described by Marzocchi *et al.* [2015] (section 2.1). In brief, the run starts in 1978 and is 30 years long, ending in 2007. It is initialized with World Ocean Atlas (WOA) 2005 climatological fields and forced with 6 hourly winds, daily heat fluxes, and monthly precipitation fields [Brodeau *et al.*, 2010]. There is moderate relaxation of the sea surface salinity fields, which are restored toward WOA 2005. Model outputs are stored as successive 5 day means throughout the model run and these are the outputs used for the particle tracking in this paper. For more details of the model setup and configuration, see Marzocchi *et al.* [2015].

Here we use 11 years of 5 day mean velocity fields (from 1997 to 2007 inclusive) to drive particle tracking in order to make a qualitative comparison with the SeaWiFS 1998–2007 observations. The reason for the extra year of model run is that particle tracking is applied in the period leading up to each year’s bloom (see section 3.1 below). An example of a 5 day velocity field from NEMO for the bloom area is shown in Figure 2 and displays a highly variable mesoscale eddy field similar to that known to exist in the bloom area [cf. Longhurst, 2001, Figure 2]. It is recognized that the mesoscale eddy field plays a key role in the development and propagation of the bloom [Longhurst, 2001; Srokosz *et al.*, 2004; Srokosz and Quartly, 2013]; therefore, it is important that the model is able to reproduce a realistic eddy field to the east of Madagascar. Marzocchi *et al.* [2015] have demonstrated that the NEMO 1/12° model produces a realistic mesoscale eddy field in the North Atlantic (their Figure 8), which gives added confidence in using the same model run here.

The Ariane package [Blanke and Raynaud, 1997] (available online at: <http://stockage.univ-brest.fr/~grima/Ariane>) is applied to the NEMO velocity field described above to track water parcels using point particles that are released into the modeled ocean circulation (cf. Popova *et al.* [2013] and Robinson *et al.* [2014], who

chlorophyll over the bloom area to the mean surface chlorophyll over an area further east, while Wilson and Qiu’s [2008] criterion for the existence of a bloom is that the chlorophyll concentration exceeds  $0.15 \text{ mg m}^{-3}$ . Here the latter criterion will be used to define the presence and extent of the bloom, and to examine its interannual variability as it allows the spatial extent of the bloom to be delineated.

### 2.1.2. Altimetric Sea Surface Currents

The satellite altimeter data used here are produced by Ssalto/Duacs and distributed by AVISO (<http://www.aviso.altimetry.fr/duacs/>) [AVISO, 2014]. A merged data product, from only two satellites at any one time, is used as this provides consistent data set appropriate for interannual variability studies. The Absolute Dynamic Topography

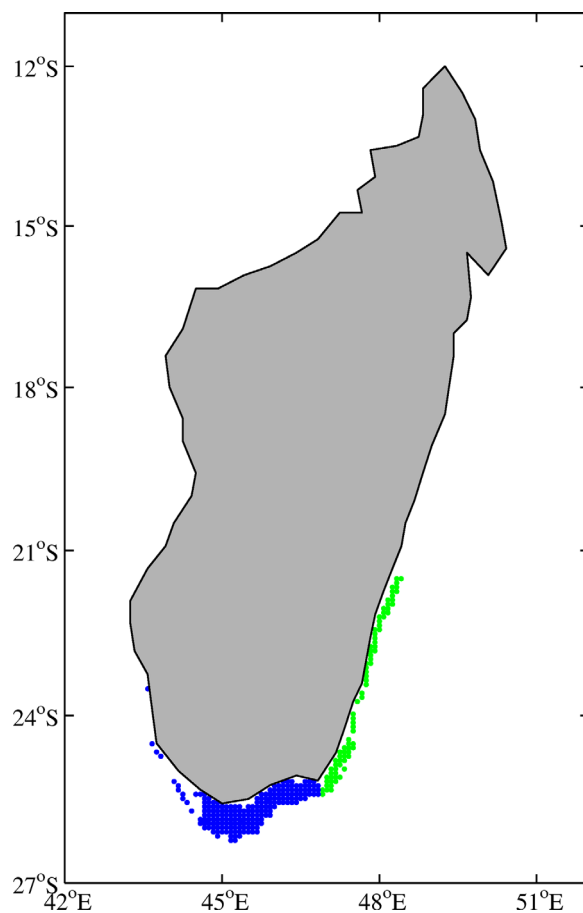


**Figure 3.** Lagrangian particle release area around Madagascar (as represented in the model grid)—differentiating particle to east (green—EMC) and south (blue—shallow shelf). A total of 275 particles are released every 5 days; of which 81 particles are released to the east and 194 particles to the south. The particles are released at the surface in the area that lies between the 50 and 300 m depth contours in the model. See text for discussion of release timings.

particles per year) and simply followed the particles from their release for 1 year to see whether advection could disperse them sufficiently to fertilize a bloom in the region to the east of Madagascar.

The second experiment was based on the assumption that the bloom would utilize all the available iron and addressed the question of whether advection could resupply iron for a bloom in the following year. In this experiment, particles were released from a nominal end of the bloom in May until January of the following year and tracked during the nine intervening months until the nominal start of the bloom in February of the following year.

A third particle-tracking experiment was also carried out to determine whether the particle released to the east of Madagascar, in the East Madagascar Current, or those released to the south of Madagascar on the shallow shelf were more likely to be advected to the east. Here the results of the second experiment were used, with the simple variation of subsetting the particles as shown in Figure 3; this results in 194 particles being released to the south and 81 to the east of Madagascar.

An important caveat to the results discussed below is that the NEMO 1/12° model, while run for specific years, will not be able to provide a direct comparison with the satellite observations for the same year. The reason for this is that the mesoscale eddy field in NEMO is not initialized to match the real-world eddy field (because of chaotic dynamics this is only possible using data assimilation). Therefore, while in a statistical sense, the model might be expected to reproduce the mesoscale eddy field behavior [see Marzocchi *et al.*, 2015], it is not expected to reproduce the exact eddy field behavior year-on-year. However, as will become

used output from a NEMO 1/4° run). The method is presented in detail and discussed by Blanke and Raynaud [1997] and Blanke *et al.* [1999].

### 3. Lagrangian Particle Tracking

#### 3.1. Methodology

In order to study the possible advection of iron, either from sediments or from riverine input, 275 particles were deployed at the surface, on the 1/12° model grid, in the area to the south and east of Madagascar where the bathymetry lies between 50 and 300 m in depth (see Figure 3). This choice is a balance between remaining close to the coast yet avoiding particles bumping into it and covering the shelf region from which iron might enter the water column [Elrod *et al.*, 2004; Dale *et al.*, 2015]. This provides sufficient particles to track in order to get a reasonable representation of their dispersal away from Madagascar.

Initially, two Lagrangian particle-tracking experiments were performed. In both experiments, the particles were released at the ocean surface. No attempt was made to distinguish between possible upwelling from sediments or input from rivers *per se*. It was simply assumed that the particles tracked were representative of iron that had entered the surface waters around Madagascar from whichever source. The first experiment released particles every 5 days each year (73 releases per year, giving a total of 20,075 particles

apparent below, this caveat does not affect the usefulness of the model results for testing the hypothesis stated in section 1.

### 3.2. Results

Consider, to begin with, the results from the first Lagrangian particle-tracking experiment. There are 275 particle starting positions spaced on the  $1/12^\circ$  grid to the east and south of Madagascar at the surface, with the region of release being bounded by the 50 and 300 m depth contours (Figure 3). Particles are released every 5 days and tracked for 1 year. During the 10 model years for which the experiment was run, it was found that in some years few particle trajectories entered the bloom area, while other years showed a significant spreading of particle trajectories into the bloom area. These initial results (not shown) indicate that Lagrangian particles released to the south and east, near to the coast of Madagascar, can be advected far enough to the east to potentially fertilize the bloom. In addition, they show that there is significant interannual variability in the Lagrangian particle trajectories and so the bloom area could be subject to an intermittent supply of iron from year-to-year. These results support the hypothesis stated at the beginning of the paper.

Having found that the advection of iron east away from Madagascar could fertilize the bloom in principle, a further question arises as to whether the bloom is terminated by the exhaustion of iron in the surface water by the phytoplankton. This question cannot be addressed directly using the NEMO  $1/12^\circ$  simulation, as it does not model iron per se. However, if the bloom is terminated by the exhaustion of iron then a question that can be addressed is: can advection resupply iron in the period between the end of one bloom and the start of the one in the following year? This corresponds to the question addressed by *Mongin et al.* [2009] for the Kerguelen bloom using a model tracer experiment. Here it is addressed using Lagrangian particle tracking. In this second experiment, the release of Lagrangian particles is restricted to the months between the end of one bloom and the start of the next, and they are tracked during the nine intervening months. For simplicity, the end of the bloom is taken to be the end of April and the start to be the beginning of February of the following year, while acknowledging that in practice there is interannual variability in the timing of both the initiation and the termination of the bloom. However, since the model does not reproduce perfectly the actual behavior in any specific year (due to chaotic dynamics as noted above) this simplification is not a problem as a qualitative, rather than quantitative, answer is all that is required from this experiment.

Figure 4 shows the results for all 10 years of the NEMO  $1/12^\circ$  model run, with the particles color coded by their release month. It can be seen that in some years, the Lagrangian particle trajectories extend sufficiently far to the east to allow iron fertilization of the bloom in the following year, even if the iron had been exhausted in the previous year. Unsurprisingly, the particles released first, at the end of the previous year's bloom in May, travel furthest generally. In contrast, the particles released last, in the January of the bloom year, are closest to Madagascar having had less time to be advected away. Note that particles are not just advected east, but also south and west, and even north into the Mozambique Channel. As expected from the first NEMO experiment, the spatial extent of the particle advection displays considerable interannual variability. This result is similar to that obtained by *Mongin et al.* [2009] for the Kerguelen bloom using model tracers.

A further qualitative comparison is shown in Figure 5. Here model year results, for 2000 and 2007, have been overlaid with the SeaWiFS chl data for the month of March in the years 2002 and 1999, using the *Wilson and Qiu* [2008] criterion for the bloom of  $0.15 \text{ mg chl m}^{-3}$ . The SeaWiFS observation years were chosen to illustrate the case of an extensive (1999) and a less extensive bloom (2002). While the model years were chosen on being the best match to the observations, as noted above (section 3.1), there is no expectation that model results will match observations on a year-by-year basis. Nevertheless, this qualitative comparison shows that the behavior of the Lagrangian particles in the model can roughly match the observed spatial extent of the bloom, even though year-by-year the model cannot reproduce the details of the bloom as it has an internally generated chaotic mesoscale eddy field that may not match that in the real world (except in a statistical sense over many realizations). Of course, a better match between the extent of the particle trajectories and the extent of the bloom might have been obtained by varying the criterion for the bloom (to a different value than  $0.15 \text{ mg chl m}^{-3}$ ) but it seemed a much more stringent test to use the independently chosen value of *Wilson and Qiu* [2008]. A further point to note from Figures 2, 4, and 5 is that the particle trajectories seem to spread further north and south than the bloom itself, a point confirmed by comparing 10 year composites of both fields (not shown). This could be an artifact of either the choice of bloom criterion or an indication that the model eddy field dispersing the particles differs somewhat from

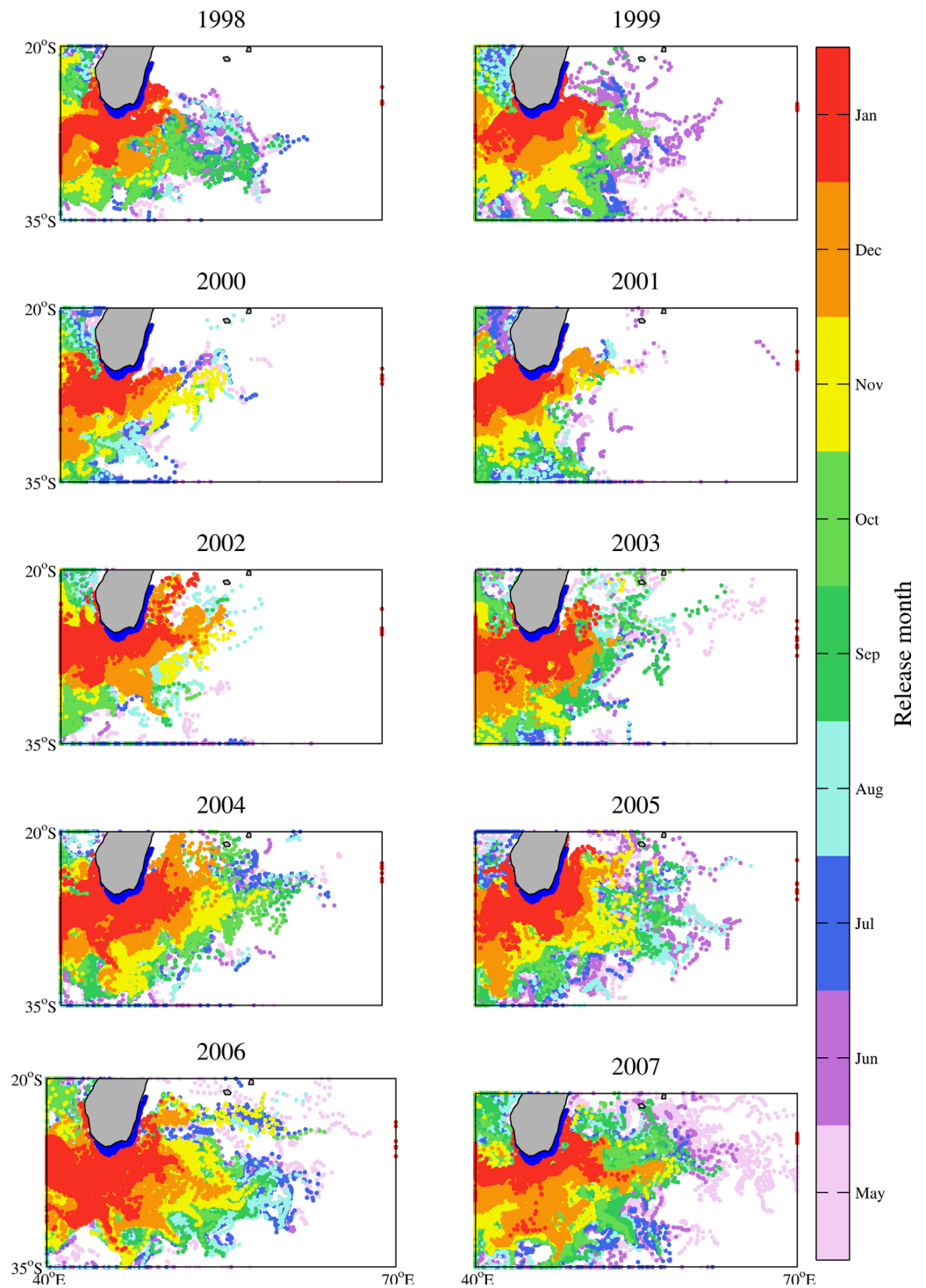


**Figure 4.** Lagrangian particle trajectories for NEMO model years 1998–2007. The blue area is where the particles are released. In this experiment, the 275 particles are released every 5 days outside the bloom period (taken as beginning of May of the previous year to the end of January of the bloom year) and tracked for the intervening 9 months. The particles are spaced  $1/12^\circ$  apart. The color scale gives the month of the particle release.

the real world, being less tightly constrained in the north-south direction (on this latter point see section 4.2 and Figure 10 below).

One question that the results so far do not answer is whether the iron would be primarily supplied from the shallow sediments to the south of Madagascar, where upwelling is known to occur [DiMarco *et al.*, 2000;

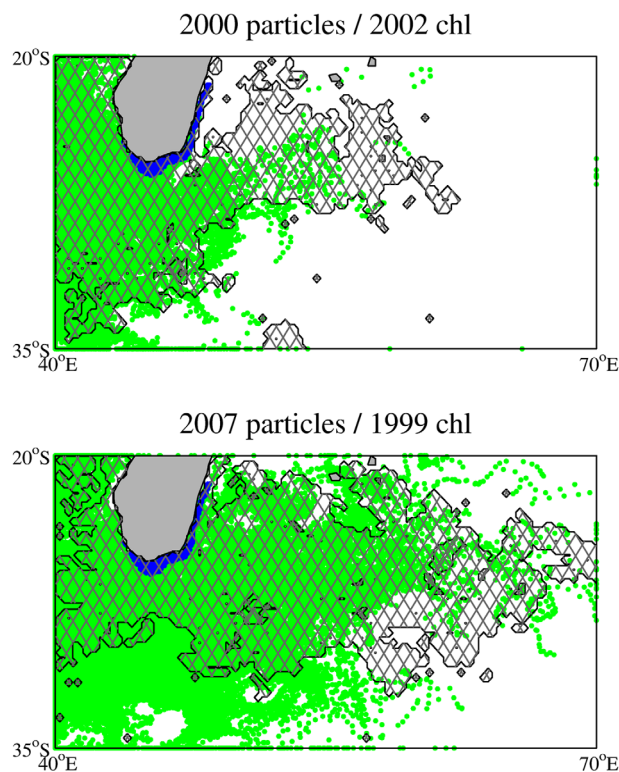


**Figure 5.** Lagrangian particle trajectories (green) for the NEMO model years (top) 2000 and (bottom) 2007. These are overlaid (hatched) with the SeaWiFS chl data for the month of March in the years 2002 and 1999, using the *Wilson and Qiu* [2008] criterion for the bloom of  $0.15 \text{ mg chl m}^{-3}$ . Note that this is only a qualitative comparison as the NEMO model is not expected to reproduce the actual mesoscale eddy field in a particular year.

*Machu et al.*, 2002], or from the east where the strong East Madagascar Current could potentially scour sediment from the sea bed? To examine this question, the particles that are released are divided into those initially lying to the east and those lying to the south (see Figure 3). Tracking the two sets of particles reveals that both areas contribute to the particles that are advected to the east away from Madagascar. However, the particles released to the east tend to contribute more to the eastward advection. In contrast, the particles released to the south tend to contribute more to advection into the Mozambique Channel (see Figures 6 and 7; note that the results shown in Figure 4 are a combination of those in these two figures). Looking at all 10 years of particle releases from the east and south, there is considerable interannual variability as to where the trajectories end up without any simple discernible pattern emerging. Therefore, no strong conclusion can be drawn regarding whether the origin of any iron being advected is to the east or the south of Madagascar—both regions potentially contribute.

Having examined the potential for iron advection using Lagrangian particle tracking, the next step is to take advantage of the NEMO  $1/12^\circ$  model output to look at the possible effects of changes in mixed layer temperatures and depths, and of the South Indian Ocean Counter-Current (SICC), on the bloom.

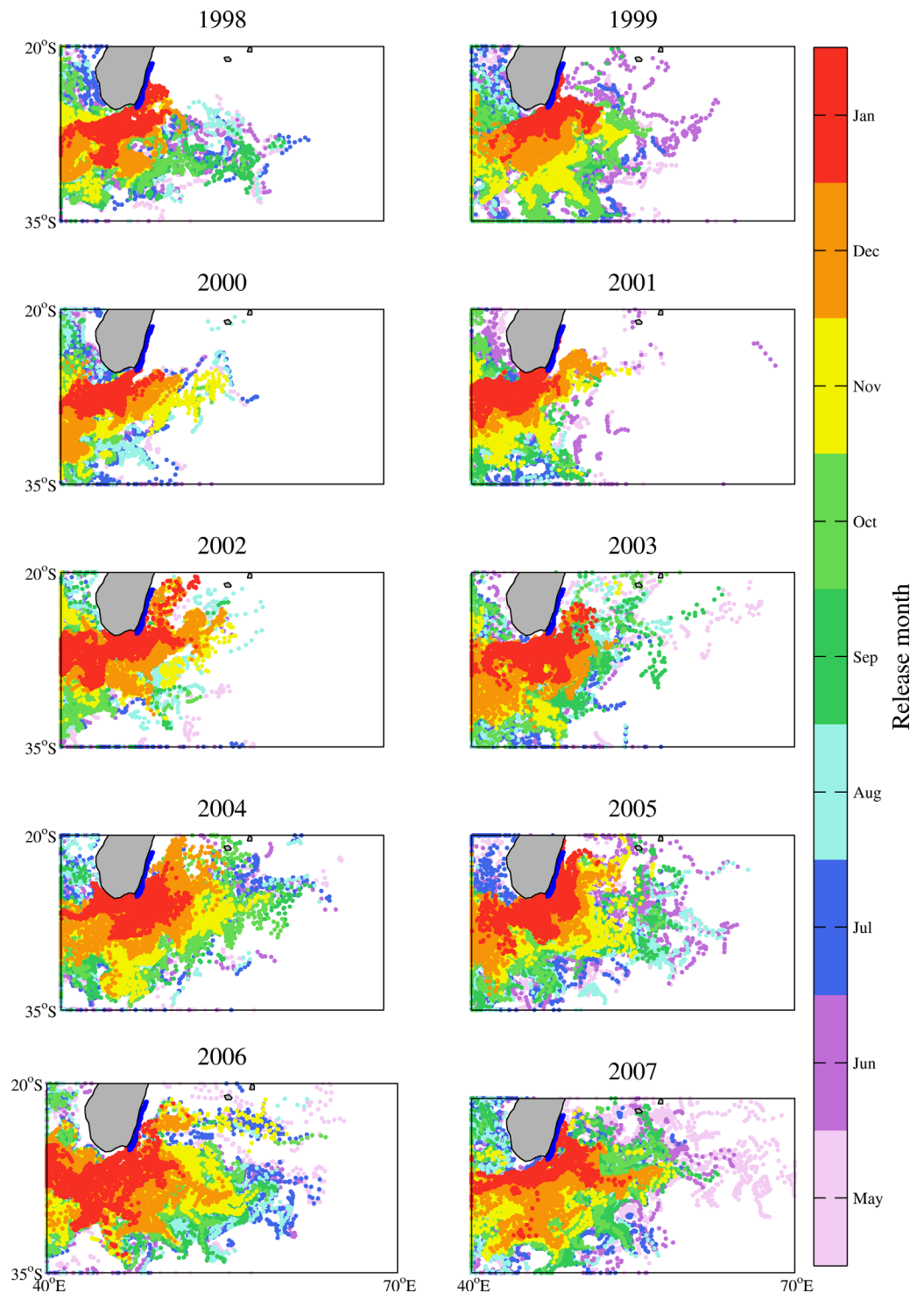
#### 4. Other Factors Affecting the Bloom

As noted by *Srokosz and Quartly* [2013, and references therein], other factors that affect the bloom are the mixed layer temperatures and depths needed to provide optimum conditions for the growth of the nitrogen fixing phytoplankton that form the bloom. *Ward et al.* [2013], in discussing diazotroph biogeography, note the preference of some species for warm temperatures and stratified, high-light environments, as found in this area in late austral summer [*Srokosz and Quartly*, 2013]. In addition, the South Indian Ocean Counter-Current (SICC) may play a role in the advection of iron, though its exact nature is disputed (see below) [*Palastanga et al.*, 2007; *Siedler et al.*, 2006; *Menezes et al.*, 2014]. Finally, the so-called Indian Ocean Dipole (IOD) may possibly influence the bloom through its effect on Indian Ocean circulation. These factors that could influence the bloom are examined next.

##### 4.1. Temperature and Mixed Layer Depth

*Wilson and Qiu* [2008, and references therein] note that nitrogen fixing *Trichodesmium*, one of the key phytoplankton species that compose the Madagascar bloom, rarely bloom below  $25^\circ\text{C}$ . *Srokosz and Quartly* [2013] (Figure 3) found from in situ observations that the bloom was confined to near-surface waters with temperatures greater than  $26.5^\circ\text{C}$ , with mixed layer depths of  $\sim 20\text{--}30$  m. Therefore, it is unlikely that the bloom will occur if the mixed layer temperature is less than  $25^\circ\text{C}$ . On examining the model output, the mixed layers are found to be relatively shallow ( $<30$  m) in the periods leading up to, during, and following

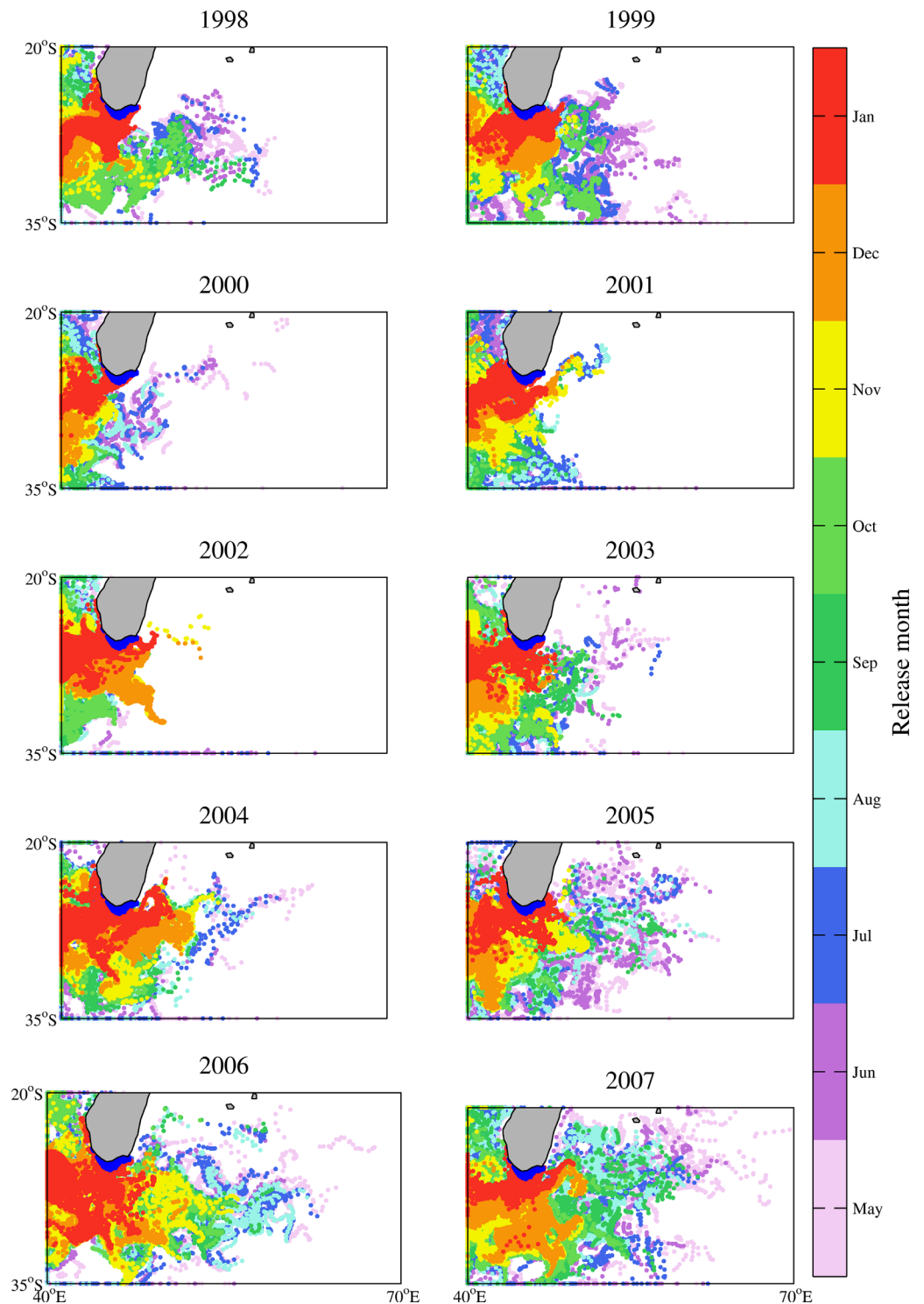




**Figure 6.** Lagrangian particle trajectories for NEMO model years 1998–2007. The blue area is where 81 particles are released every 5 days. This experiment is identical to that shown in Figure 4 but with the release of the particles restricted to the east of Madagascar in the area of the East Madagascar Current that runs south along the coast. The color scale gives the month of the particle release.

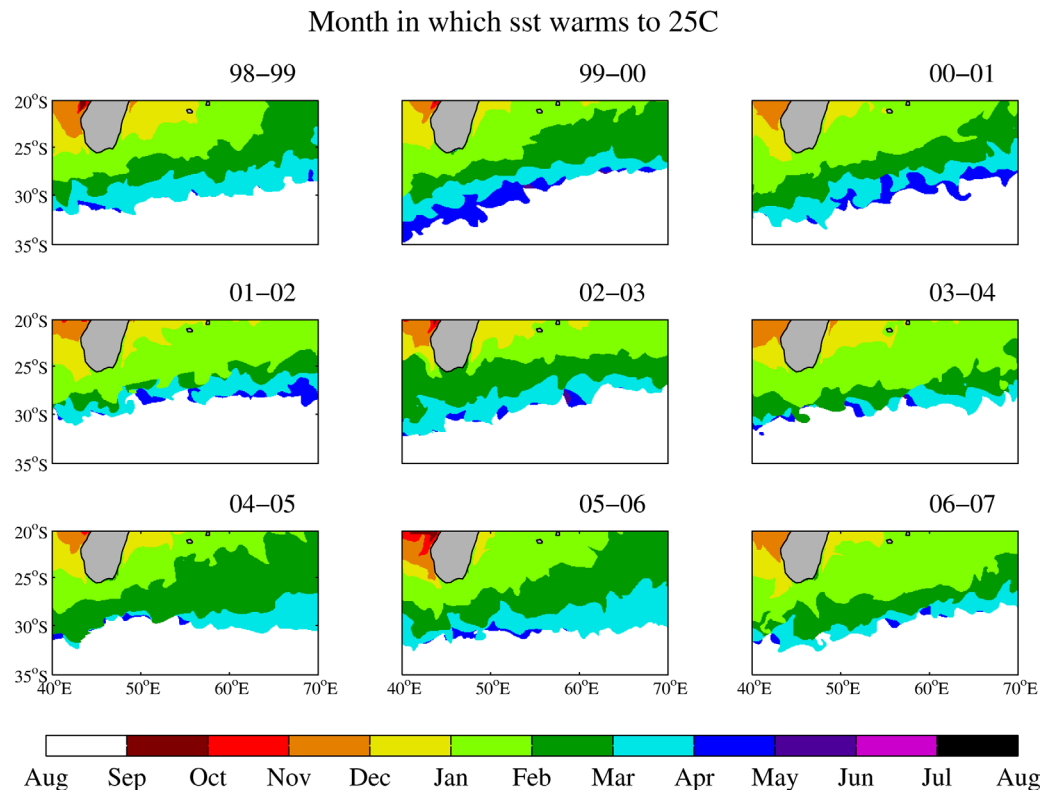
the bloom. Therefore, it seems doubtful that light limitation plays a role in its initiation and termination. However, the mixed layer temperatures may do so, so these are examined next.

Figure 8 shows results from the NEMO 1/12° ocean model for the months in which surface temperature (representative of the mixed layer temperature) exceeds 25°C, leading up to the bloom period. In contrast,



**Figure 7.** Lagrangian particle trajectories for NEMO model years 1998–2007. The blue area is where 194 particles are released every 5 days. This experiment is identical to that shown in Figure 4 but with the release of the particles restricted to the south of Madagascar in the upwelling area on the shelf. The color scale gives the month of the particle release.

Figure 9 shows when the surface temperature cools to 25°C, after the bloom period. In both figures, interannual variability can be seen in the spatial structure of the warming and cooling. For the bloom region, the surface waters warm to 25°C around January/February each year (Figure 8). In the postbloom period, the surface temperature drops below 25°C around June/July. These results suggest that the initiation of the



**Figure 8.** Results from NEMO showing the month in which surface temperatures exceed 25°C prior to the bloom period over the decade of model output examined. Note that in the white area, the temperatures never exceed 25°C.

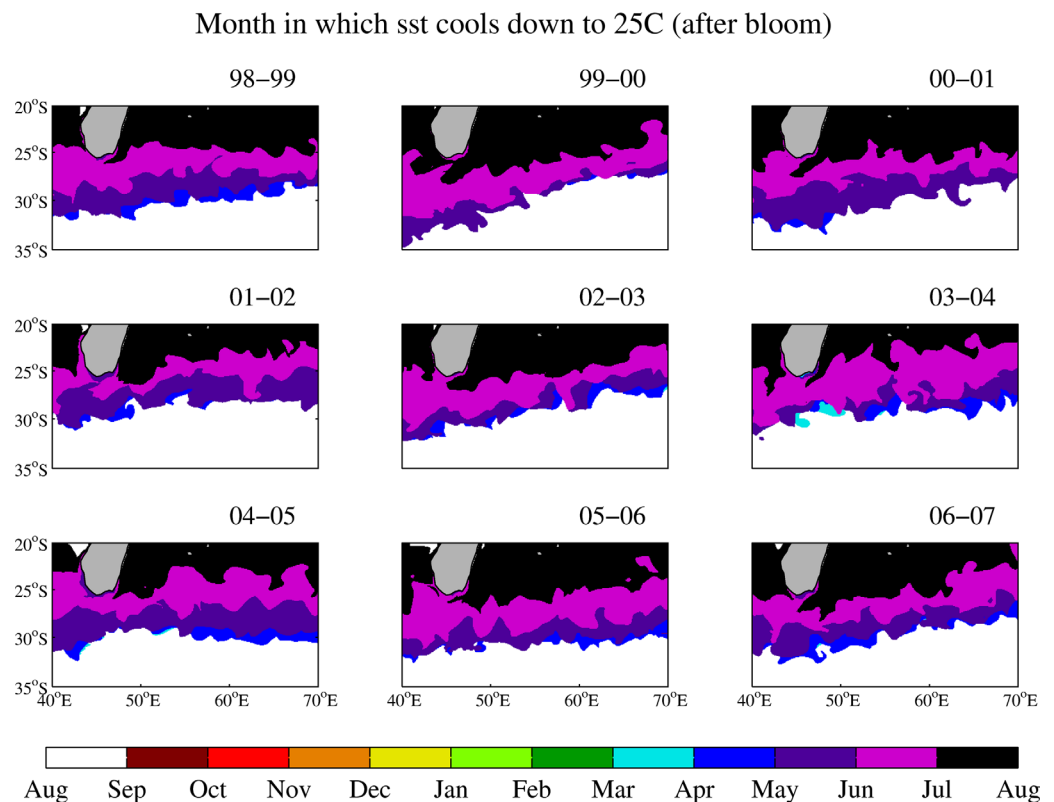


**Figure 9.** Results from NEMO showing the month in which surface temperatures drop below 25°C after the bloom period over the decade of model output examined. Note that in the white area, the temperatures never exceed 25°C, so cannot drop back below 25°C either.

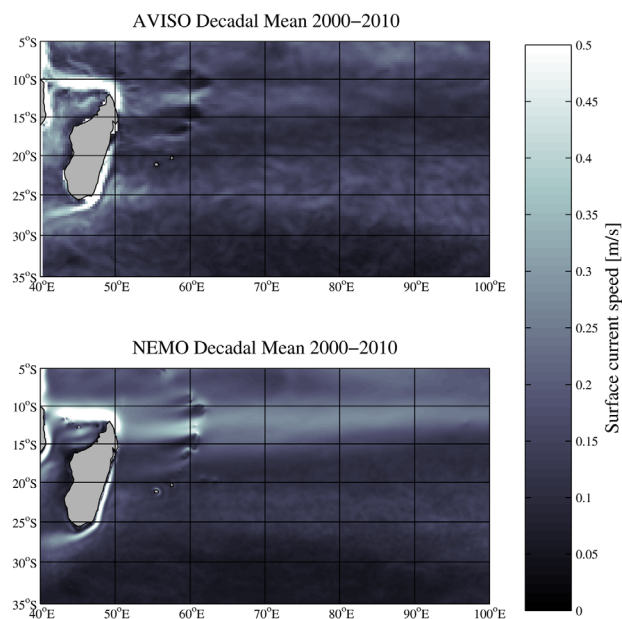


**Figure 10.** (top) Ten year (1998–2007) average of AVISO sea surface geostrophic current speeds, and a (bottom) 10 year (1998–2007) average of 1/12° NEMO sea surface current speed.

flowing eastward at approximately 25°S [Palastanga *et al.*, 2007], may play a role in the development and propagation of the Madagascar Bloom. One way that the existence of the SICC has been inferred is by averaging altimetric sea surface geostrophic currents over a number of years [Siedler *et al.*, 2006]. Here the 10 year (1998–2007) average of AVISO produced altimetric sea surface geostrophic current speeds is compared to the corresponding 10 year (1998–2007) average of 1/12° NEMO surface current speeds.

The results of comparing AVISO and NEMO surface currents are shown in Figure 10 and there is agreement generally, in line with similar comparisons by Marzocchi *et al.* [2015] for the North Atlantic (their Figure 8). The NEMO results are somewhat smoother overall and the residual variability in the 25°S band, on which the bloom is centered, slightly weaker. Both the AVISO and NEMO results show the existence of the East Madagascar Current flowing south along the east coast of Madagascar, then turning west to flow toward South Africa. Note that once the current leaves the Madagascar coast it interacts with the meso-scale eddy field and is less well defined. There is no clear evidence for the existence of the SICC in either the altimetry or the NEMO decadal means. Therefore, it can be concluded that the existence of the SICC is not necessary for iron advection to fertilize the bloom. The presence of the mesoscale eddy field (see Figure 2) is sufficient to transport particles, and therefore iron, east away from Madagascar. The averaging period used by Siedler *et al.* [2006], August 2001 to May 2006, was also examined for the AVISO data and their Figure 1c reproduced (not shown), which appears to show the existence of the SICC. This seems at odds with our 10 year average which shows no SICC but this simply indicates that caution is required both in the choice of averaging period and in the interpretation of the results obtained from altimetry (see discussion in Schlax and Chelton [2008]). More recently, Menezes *et al.* [2014], based on Argo and hydrographic observations, have suggested that the SICC has a three-branched structure, three distinct eastward flowing jets that they denote as northern, central, and southern SICC. Therefore, the exact structure of the SICC seems to be a matter of some uncertainty at present but it is beyond the scope of this paper to pursue this question.

#### 4.3. Indian Ocean Dipole (IOD)

Given the importance of the Indian Ocean Dipole [Saji *et al.*, 1999] for the Indian Ocean Circulation [Schott *et al.*, 2009], its possible role in the interannual variability of the Madagascar bloom is considered briefly here. Over the period studied here (1998–2007), the variability in the IOD dipole mode index seems to have no clear relationship to the behavior of the bloom from year-to-year. Indeed, over this period, the IOD mode index exhibits low variability except in 1998 (negative) and 2006 and 2007 (positive). The lack of a

bloom could be triggered by the rise in the temperature of the surface water, as the mixed layer shallows. In contrast, from examining the model mixed layer depths (not shown), it would appear that the termination of the bloom is unlikely to be caused by either mixed layer deepening (for the bloom area it is never deep enough for light limitation to come into play) or by cooling as this occurs much later than the observed timing of the termination of the bloom (Figure 9).

These results are suggestive but not conclusive regarding the possible causes of the initiation and termination of the bloom and will be discussed further in section 5 (below).

#### 4.2. South Indian Ocean Counter-Current (SICC) and Eddy Field

It has been suggested by Wilson and Qiu [2008] and Huhn *et al.* [2012] that the SICC, a shallow (~200 m deep) current

relationship between the bloom and the IOD might be considered unsurprising as the impacts of the IOD on the circulation are seen primarily in the tropical Indian Ocean [Schott *et al.*, 2009]. Previously, Srokosz *et al.* [2004] found no obvious link in this area to meteorological parameters (winds and fluxes) and Uz [2007] had concluded that the interannual variability did not correlate well with any obvious physical parameter. Likewise, the modeling and satellite observations study of Currie *et al.* [2013] shows no indication of IOD (or ENSO) influence on chlorophyll anomalies to the east of Madagascar, though their model does lack nitrogen fixers. Finally, Longhurst [2007] also noted the lack of any relationship between the bloom and climatic indices more generally. Consequently, the role of the IOD is not considered any further here.

## 5. Conclusions

The original hypothesis of this paper was that: iron from sediments around Madagascar is advected east by the mesoscale eddy field to fertilize the bloom, and the variability in the advection explains the significant interannual variability in the spatial extent of the bloom. The Lagrangian particle tracking results using NEMO 1/12° ocean model output (described in section 3) support this hypothesis by showing that iron could be advected east by the mesoscale eddy field in the nonbloom period to support a bloom in the following year. Furthermore, the model results show sufficient interannual variability in the spatial extent of the Lagrangian particle advection to explain the observed interannual variability in the spatial extent of the SeaWiFS ocean color observations of the bloom. The results also show (section 4.2) that the existence of the SICC is not necessary to explain either the extent or the interannual spatial variability of the bloom. The exact nature and form of the SICC seem unclear [Palastanga *et al.*, 2007; Siedler *et al.*, 2006; Menezes *et al.*, 2014] but it is not necessary to solve these problems here, as the conclusions are not dependent on doing so.

From the numerical experiments presented in this paper, it is not possible to distinguish between iron advection from sediments and iron advection from riverine input [Uz, 2007; Srokosz and Quartly, 2013]. Both would enter the surface waters and be advected east. However, as noted by Srokosz and Quartly [2013], most of the major Madagascan rivers drain into the Mozambique Channel well away from the area of Lagrangian particle release (see Figure 3), so iron from sediments seems a more likely source (by analogy with Kerguelen and Crozet) [see Blain *et al.*, 2007; Pollard *et al.*, 2009]. Jeandel *et al.* [2011] note that 23 times more iron could reach the ocean from margin sources than that supplied by river fluxes. Only future in situ measurements are likely to be able to distinguish between these two possible sources of iron (possibly through the use of isotopic composition measurements) [Jeandel *et al.*, 2011].

In addition to its use for Lagrangian particle tracking, the model output has also been examined to see whether it might give further insight into physical factors that could affect the initiation and termination of the bloom. The nitrogen fixing phytoplankton that compose the bloom are known to be sensitive to temperature and to require a relatively shallow mixed layer [Srokosz and Quartly, 2013; Ward *et al.*, 2013; Wilson and Qiu, 2008, and references therein]. The model results (section 4.1) show that the interannual variability of mixed layer temperatures over the bloom area could explain the interannual variability in the timing of the initiation but not the termination of the bloom. The initiation of the bloom could be due to the warming of the surface waters leading to optimal conditions for the growth of the nitrogen fixing phytoplankton. Thereafter the termination of the bloom could be due to the exhaustion of iron by the phytoplankton as the bloom develops, since the model results suggest that the surface waters do not start to cool until after the bloom terminates. Again in situ observations of iron are required to confirm, or otherwise, that this is the case.

In summary, the picture that emerges from the above analysis is that the Madagascar bloom is fertilized by iron advected east from the island. The bloom is initiated in the late austral summer, when the upper ocean is depleted of nitrate due to the prior spring bloom, and the conditions (mixed layer temperatures) become suitable for nitrogen fixing phytoplankton to flourish. The bloom is terminated by the exhaustion of iron. This picture potentially explains both the interannual variability in the spatial extent of the bloom and of the timing of its initiation and termination. As noted above, this picture can only be confirmed (or disproved) by making further in situ measurements of the bloom, and particularly of iron availability for which no data are extant for this region.

**Acknowledgments**

M.A.S. is grateful to Alex Poulton for discussions regarding nitrogen fixers and the Madagascar Bloom. SeaWiFS data were obtained from NASA (<http://oceansci.gsfc.nasa.gov/SeaWiFS/L3SMI/>). Altimeter products were produced by Aviso/Duacs and distributed by Aviso, with support from CNES (<http://www.aviso.oceanobs.com/duacs/>). The study was carried out using the computational tool Ariane, developed by B. Blanke and N. Grima. The 1/12° NEMO simulation used in this work was produced using the ARCHER UK National Supercomputing Service (<http://www.archer.ac.uk>). This work was funded by the UK Natural Environment Research Council, in part through a PhD studentship for J.R. (NE/K500938/1) and national capability funding for M.A.S., E.E.P., and A.Y. It builds on the work of H.M. during her master's studies at the National Oceanography Centre (2013–2014).

**References**

AVISO (2014), *SSALTO/DUACS User Handbook: (M)SLA and (M)ADT Near-Real Time and Delayed Time Products, CLS-DOS-NT-06-034, SALP-MU-P-EA-21065-CLS*, 59 pp., Cent. Natl. D'études Spatiales, Ramonville St Agne, France. [Available at [http://www.aviso.altimetry.fr/fileadmin/documents/data/tools/hdbk\\_duacs.pdf](http://www.aviso.altimetry.fr/fileadmin/documents/data/tools/hdbk_duacs.pdf).]

Blain, S., et al. (2007), Effect of natural iron fertilisation on carbon sequestration in the Southern Ocean, *Nature*, *446*, 1070–1075.

Blanke, B., and S. Raynaud (1997), Kinematics of the Pacific Equatorial Undercurrent: An Eulerian and Lagrangian approach from GCM results, *J. Phys. Oceanogr.*, *27*, 1038–1053.

Blanke, B., M. Arhan, G. Madec, and S. Roche (1999), Warm water paths in the equatorial Atlantic as diagnosed with a general circulation model, *J. Phys. Oceanogr.*, *29*, 2753–2768.

Brodeau, L., B. Barnier, A.-M. Treguier, T. Penduff, and S. Gulev (2010), An ERA40-based atmospheric forcing for global ocean circulation models, *Ocean Model.*, *31*, 88–104.

Currie, J. C., M. Lengaigne, J. Vailard, D. M. Kaplan, O. Aumont, S. W. A. Naqvi, and O. Maury (2013), Indian Ocean Dipole and El Niño/Southern Oscillation impact on regional chlorophyll anomalies in the Indian Ocean, *Biogeosciences*, *10*, 6677–6698.

Dale, A. W., L. Nickelsen, F. Scholz, C. Hensen, A. Oschlies, and K. Wallman (2015), A revised global estimate of dissolved iron fluxes from marine sediments, *Global Biogeochem. Cycles*, *29*, 691–707, doi:10.1002/2014GB005017.

DiMarco, S. F., P. Chapman, and W. D. Nowlin (2000), Satellite observations of upwelling on the continental shelf south of Madagascar, *Geophys. Res. Lett.*, *27*, 3965–3968.

Dufois, F., N. J. Hardman-Mountford, J. Greenwood, A. J. Richardson, M. Feng, S. Herbet, and R. Matear (2014), Impact of eddies on surface chlorophyll in the South Indian Ocean, *J. Geophys. Res.*, *119*, 8061–8077, doi:10.1002/2014JC010164.

Elrod, V. A., W. M. Berelson, K. H. Coale, and K. S. Johnson (2004), The flux of iron from continental shelf sediments: A missing source for global budgets, *Geophys. Res. Lett.*, *31*, L12307, doi:10.1029/2004GL020216.

Gaube, P., D. B. Chelton, P. G. Strutton, and M. J. Behrenfeld (2013), Satellite observations of chlorophyll, phytoplankton biomass, and Ekman pumping in nonlinear mesoscale eddies, *J. Geophys. Res.*, *118*, 6349–6370, doi:10.1002/2013JC009027.

Gaube, P., D. J. McGillicuddy Jr., D. B. Chelton, M. J. Behrenfeld, and P. G. Strutton (2014), Regional variations in the influence of mesoscale eddies on near-surface chlorophyll, *J. Geophys. Res.*, *119*, 8195–8220, doi:10.1002/2014JC010111.

Huhn, F., A. von Kameke, V. Pérez-Muñuzuri, M. J. Olascoaga, and F. J. Beron-Vera (2012), The impact of advective transport by the South Indian Ocean countercurrent on the Madagascar bloom, *Geophys. Res. Lett.*, *39*, L06602, doi:10.1029/2012GL051246.

Jeandel, C., B. Peucker-Ehrenbrink, M. T. Jones, C. R. Pearce, E. H. Oelkers, Y. Godderis, F. Lacan, O. Aumont, and T. Arsouze (2011), Ocean margins: The missing term in the oceanic element budgets?, *Eos Trans. AGU*, *92*, 217–224.

Longhurst, A. (2001), A major seasonal phytoplankton bloom in the Madagascar Basin, *Deep Sea Res., Part 1*, *48*, 2413–2422.

Longhurst, A. R. (2007), *The Ecological Geography of the Sea*, 2nd ed., Academic.

Machu, E., J. R. E. Lutjeharms, A. M. Webb, and H. van Aken (2002), First hydrographic evidence of the southeast Madagascar upwelling cell, *Geophys. Res. Lett.*, *29*(21), 2009, doi:10.1029/2002GL015381.

Madec, G. (2008), NEMO reference manual, ocean dynamic component: NEMO-OPA, Notes du pole de modelisation, *Tech. Rep. 27*, Inst. Pierre Simon Laplace, Paris, France.

Marzocchi, A., J. J.-M. Hirschi, N. P. Holliday, S. A. Cunningham, A. T. Blaker, and A. C. Coward (2015), The North Atlantic subpolar circulation in an eddy-resolving global ocean model, *J. Mar. Syst.*, *142*, 126–143.

Menezes, V. V., H. E. Phillips, A. Schiller, N. L. Bindoff, C. M. Domingues, and M. L. Vianna (2014), South Indian countercurrent and associated fronts, *J. Geophys. Res. Oceans*, *119*, 6763–6791, doi:10.1002/2014JC010076.

Mongin, M. M., E. R. Abraham, and T. W. Trull (2009), Winter advection of iron can explain the summer phytoplankton bloom that extends 1000km downstream of the Kerguelen Plateau in the Southern Ocean, *J. Mar. Res.*, *67*, 225–237.

Monteiro, F. M., M. J. Follows, and S. Dutkiewicz (2010), Distribution of diverse nitrogen fixers in the global ocean, *Global Biogeochem. Cycles*, *24*, GB3017, doi:10.1029/2009GB003731.

NASA (2009), *Ocean Colour Observations: Product Level Descriptions*. [Available at [http://oceancolor.gsfc.nasa.gov/PRODUCTS/product\\_level\\_desc.html](http://oceancolor.gsfc.nasa.gov/PRODUCTS/product_level_desc.html).]

Palastanga, V., P. J. van Leeuwen, M. W. Schouten, and W. P. M. de Ruijter (2007), Flow structure and variability in the subtropical Indian Ocean: Instability of the South Indian Counter Current, *J. Geophys. Res.*, *112*, C01001, doi:10.1029/2005JC003395.

Pollard, R. T., et al. (2009), Southern Ocean deep-water carbon export enhanced by natural iron fertilisation, *Nature*, *457*, 577–581.

Popova, E. E., A. Yool, Y. Aksenov, and A. C. Coward (2013), Role of advection in Arctic Ocean lower trophic dynamics: A modeling perspective, *J. Geophys. Res. Oceans*, *118*, 1571–1586, doi:10.1002/jgrc.20126.

Poulton, A. J., M. C. Stinchcombe, and G. D. Quartly (2009), High numbers of *Trichodesmium* and diazotrophic diatoms in the southwest Indian Ocean, *Geophys. Res. Lett.*, *36*, L15610, doi:10.1029/2009GL039719.

Robinson, J., E. E. Popova, A. Yool, M. Srokosz, R. S. Lampitt, and J. R. Blundell (2014), How deep is deep enough? Ocean iron fertilization and carbon sequestration in the Southern Ocean, *Geophys. Res. Lett.*, *41*, 2489–2495, doi:10.1002/2013GL058799.

Saji, N. H., B. N. Goswami, P. N. Vinayachandran, and T. Yamagata (1999), A dipole mode in the tropical Indian Ocean, *Nature*, *401*, 360–363.

Schlx, M. G., and D. B. Chelton (2008), The influence of mesoscale eddies on the detection of quasi-zonal jets in the ocean, *Geophys. Res. Lett.*, *35*, L24602, doi:10.1029/2008GL035998.

Schott, F. A., S.-P. Xie, and J. P. McCreary (2009), Indian Ocean Circulation and climate variability, *Rev. Geophys.*, *47*, RG1002, doi:10.1029/2007RG000245.

Siedler, G., M. Rouault, and J. R. E. Lutjeharms (2006), Structure and origin of the subtropical South Indian Ocean Countercurrent, *Geophys. Res. Lett.*, *33*, L24609, doi:10.1029/2006GL027399.

Srokosz, M. A., and G. D. Quartly (2013), The Madagascar Bloom: A serendipitous study, *J. Geophys. Res. Oceans*, *118*, 14–25, doi:10.1029/2012JC008339.

Srokosz, M. A., G. D. Quartly, and J. J. H. Buck (2004), A possible plankton wave in the Indian Ocean, *Geophys. Res. Lett.*, *31*, L13301, doi:10.1029/2004GL019738.

Uz, B. M. (2007), What causes the sporadic phytoplankton bloom south-east of Madagascar?, *J. Geophys. Res.*, *112*, C09010, doi:10.1029/2006JC003685.

Ward, B. A., S. Dutkiewicz, C. M. Moore, and M. J. Follows (2013), Iron, phosphorus, and nitrogen supply ratios define the biogeography of nitrogen fixation, *Limnol. Oceanogr. Methods*, *58*, 2059–2075.

Wilson, C., and X. Qiu (2008), Global distribution of summer chlorophyll blooms in oligotrophic gyres, *Prog. Oceanogr.*, *78*, 107–134.